Application of the Variational Approach for the Computation of Forces around a Wing and Comparison with other Methods

Daniel Diaz[1]*, Bartosz Protas[2], Frédéric Pons[1], Laurent David[1]

[1]Institut Pprime, CNRS, Université de Poitiers, ENSMA, France

[2]Department of Mathematics and Statistics, McMaster University, Hamilton, Ont., Canada

*daniel.diaz@univ-poitiers.fr

Abstract

In this paper we present an application of the variational approach introduced by Protas et al. (2000), which requires only the velocity fields and its derivatives to determine forces generated around a body. First, the approach is presented and adapted for our 3D test problem. The obtained expression for the hydrodynamic force involves a harmonic function η, whose determination is also shown. Then, numerical flow fields obtained with LES are used in order to evaluate the influence of different parameters on the forces and to offer a validation of the proposed approach. This allows us to assess the accuracy of the method and its advantages.

Next, a comparison of the proposed variational approach with the momentum equation approach presented by David et al (2009) is discussed. The momentum equation approach offers a non-intrusive method to determine the forces, but it requires the pressure field around the object. On the other hand, the variational approach requires the determination of the vorticity field on the surface of the wing, which is not always trivial to obtain with sufficient accuracy, but it does not need the pressure field. This paper aims to compare both methods and show their relative advantages and sensitivities to different parameters for a 3D flow around a NACA0015 airfoil.

1 Introduction

The non-intrusive determination of the aerodynamic forces experience by a body has become an important topic of research in the last years. Low Reynolds cases that involve slight forces, such as the flow around micro-air vehicles (MAVs), need the use of these non-intrusive methods to obtain reliable results.

Noca et al. (1997) introduced the first non-intrusive method discussed in this paper, which deduces the unsteady forces from velocity flow fields by the application of the momentum equation to a control volume around the body. This method allows the determination of steady, van Oudheusden et al. (2006), and unsteady, Kurtulus et al. (2007), aerodynamic forces. Moreover, David et al. (2009) developed some practical applications of the approach for numerical and experimental data. Nevertheless, the momentum equation approach has its drawbacks (pressure term), what results in the need to develop new non-intrusive methods. Protas et al. (2000) evaluated the effectiveness of the variational approach initially proposed by Quartapelle et al. (1983).

In this paper, we focus on the application of the variational approach to a 3D case and the influence of different parameters such as the spatial resolution and the size of the integration domain. Then, a comparison between the variational and the momentum equation approaches will be presented, leading to a concluding discussion.

2   Force determination methods

- **Momentum equation approach**

Thanks to the determination of the velocity and acceleration fields by Time-Resolved Particle Image Velocimetry (TR-PIV), the application of the momentum equation is possible. The equation in the integral form provides with the instantaneous forces $\vec{F}(t)$ experienced by the body, which consists of four terms,

$$\vec{F}(t) = -\rho \iiint_V \frac{\partial \vec{V}}{\partial t} dV - \rho \iint_S (\vec{V} \cdot \vec{n})(\vec{V} - \vec{V_s}) dS - \iint_S p\vec{n}\, dS + \iint_S \bar{\bar{\tau}} \cdot \vec{n}\, dS \qquad (1)$$

$$\underset{\substack{\text{Unsteady} \\ \text{Term}}}{} \qquad \underset{\substack{\text{Convective} \\ \text{Term}}}{} \qquad \underset{\substack{\text{Pressure} \\ \text{Term}}}{} \qquad \underset{\substack{\text{Viscous} \\ \text{Term}}}{}$$

where $\vec{n}$ is the normal to the control surface S as shown in figure 1, ρ is the fluid density, $\vec{V}$ is the fluid velocity vector, $\vec{V_s}$ is the control volume velocity and $\bar{\bar{\tau}}$ is the viscous stress tensor.
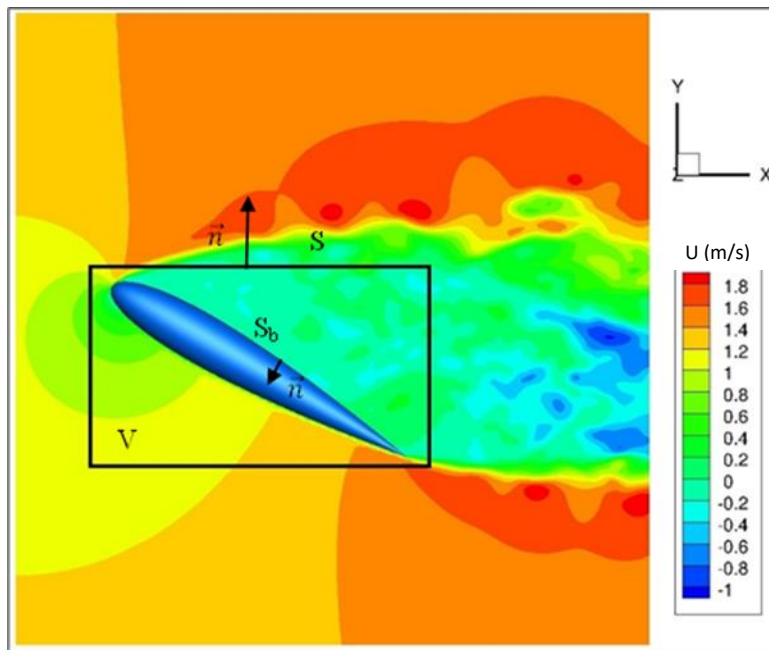

Figure 1: Control volume representation for the momentum equation approach.

The unsteady and convective terms can be directly computed from the TR-PIV velocity flow fields. The third term presents the need to calculate the pressure along the control surface, which

constitutes the main disadvantage of this method. This parameter is obtained by spatially integrating the pressure gradient derived from the velocity flow field:

$$\frac{D\vec{V}}{Dt} = -\frac{1}{\rho}\nabla p + \nu\nabla^2\vec{V} \tag{2}$$

The determination of the pressure by numerical integration induces error propagation, that comes from measurement error, round-off error and integration algorithm errors, which may end in unreliable results. However, the methods to resolve the pressure from the velocity fields have improved significantly. Nonetheless, if only the determination of the forces is needed, an approach that does not require the demanding task of the pressure computation would be more efficient.

Finally, the viscous term represents the action of the viscous stresses around the control volume and it is deduced form the following expression:

$$\bar{\bar{\tau}} = \mu\big(\vec{\nabla}\otimes\vec{V} + \vec{\nabla}\otimes\vec{V}^t\big) \tag{3}$$

- **Variational approach**

As previously introduced, Quartapelle et al. (1983) proposed the variational approach to determine the instantaneous forces without calculating the pressure. This method is derived by formulating the pressure contribution to the force in a manner that only the velocity and vorticity are needed to compute it.

By definition, the pressure and viscous contribution to the force can be written as:

$$\vec{F} = \overrightarrow{F^P} + \overrightarrow{F^\mu} = -\oint_{\partial\Omega}\big(-p\vec{n} + \bar{\bar{\Pi}}_\mu \cdot \vec{n}\big)\,\mathrm{d}\sigma \tag{4}$$

$$\bar{\bar{\Pi}}_\mu = \mu\left[\nabla\vec{V} + \big(\nabla\vec{V}\big)^T\right] \tag{5}$$
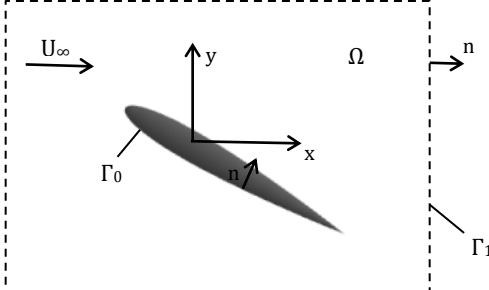(for incompressible Newtonian fluids)

Applying the identity of vector calculus and having a divergence-free velocity field $\big(\nabla\vec{V} = 0\big)$, the vorticity appears in the force equation:

$$\oint_{\partial\Omega}\big(\nabla\vec{V}\big)^T \cdot \vec{n}\,\,\mathrm{d}\sigma = \int_\Omega \nabla\big(\nabla\cdot\vec{V}\big)\,\,\mathrm{d}\Omega \tag{6}$$

$$\vec{F} = \oint_{\partial\Omega}\left[p\vec{n} - \mu\big(\nabla\vec{V} + \big(\nabla\vec{V}\big)^T\big)\cdot\vec{n}\right]\mathrm{d}\sigma = \oint_{\partial\Omega}\left[p\vec{n} - \mu\big(\nabla\vec{V} - \big(\nabla\vec{V}\big)^T\big)\cdot\vec{n}\right]\mathrm{d}\sigma$$

$$\vec{F} = \oint_{\partial\Omega}[p\vec{n} + \mu(\vec{n}\times\vec{\omega})]\,\mathrm{d}\sigma \tag{7}$$

Following the idea proposed by Protas et al. (2000), we will consider the region Ω, which corresponds to a control volume around the object. It is limited by two surfaces: Γ_0, which coincides with the surface of the body, and Γ_1, that is the outer surface. Continuing with the proposed idea, a function η_x that only depends on the geometry of the body is defined:

$$\Delta\eta_x = 0 \qquad\qquad in\ \Omega$$
$$\vec{n}\cdot\nabla\eta_x = -\overrightarrow{e_x}\cdot\vec{n} \qquad at\ \Gamma_0 \qquad (8)$$
$$\vec{n}\cdot\nabla\eta_x = 0 \qquad\qquad at\ \Gamma_1$$

Figure 2: Scheme of the object and the control volume to show the boundary conditions of η_x.

The function η_x is used for the determination of the X-component of the force. Similarly, the functions η_y and η_z are defined for the computation of the other two components of the force.

The introduction of this function allows the modification of the pressure term in the force equation. First, an expression for the pressure is obtained from the Navier-Stokes equations:

$$-\nabla p = \rho\frac{\partial\vec{V}}{\partial t} + \rho(\vec{V}\cdot\nabla)\vec{V} + \rho\mu\nabla\times\omega \qquad (9)$$

It is then projected, Protas et al. (2000), in the sense of the Hilbert space L_2 (Ω) on the gradient $\nabla\eta_x$. The terms in equation (9) are multiplied by $\nabla\eta_x$, and then integrated over Ω. Integrating by parts, using the incompressibility constraint and the boundary conditions for η_x, the following expression for the pressure contribution to the X-component of the force is derived, where $n_x = \overrightarrow{e_x}\cdot\vec{n}$:

$$F_x^P = \oint_{\Gamma_0} (n_x p)\,d\sigma$$
$$(10)$$
$$F_x^P = \rho\oint_{\Gamma_0\cup\Gamma_1} \eta_x\vec{n}\cdot\left(\frac{\partial\vec{V}}{\partial t}\right)d\sigma + \rho\oint_{\Gamma_0\cup\Gamma_1}\vec{n}\cdot(\vec{\omega}\times\nabla\eta_x)\,d\sigma + \rho\int_\Omega \nabla\eta_x\cdot[(\vec{V}\cdot\nabla)\vec{V}]\,d\Omega$$

Adding the contribution of the viscosity, the equation for the X-component of the force is:

$$F_x = \rho\oint_{\Gamma_0\cup\Gamma_1}\eta_x\vec{n}\cdot\left(\frac{\partial\vec{V}}{\partial t}\right)d\sigma + \rho\oint_{\Gamma_0\cup\Gamma_1}\vec{n}\cdot(\vec{\omega}\times\nabla\eta_x)\,d\sigma$$
$$+\rho\int_\Omega\nabla\eta_x\cdot[(\vec{V}\cdot\nabla)\vec{V}]\,d\Omega + \oint_{\Gamma_0}\mu(\vec{n}\times\vec{\omega})\,d\sigma \qquad (11)$$

- **Numerical data application**

The data base used to test the methods of study comes from an Improved Delayed Detached Eddy Simulation (IDDES). The flow around a NACA0015 profile with an 80mm cord and 140mm span is

considered. The wing has an angle of attack of 30 degrees and the upstream velocity is fixed to U_∞=1.25m/s. The velocity fields are exported into a cartesian grid with a spatial resolution of 1mm and a sampling rate of 4000Hz.

As previously explained, the η functions depend only on the geometry of the body, therefore they have to be determined for the objects tested. Figure 3 shows the η functions for the wing used for the numerical simulations. Notice that as a section in the middle of the wing is shown where the Z-component of the normal is zero, the function η_z is also null.
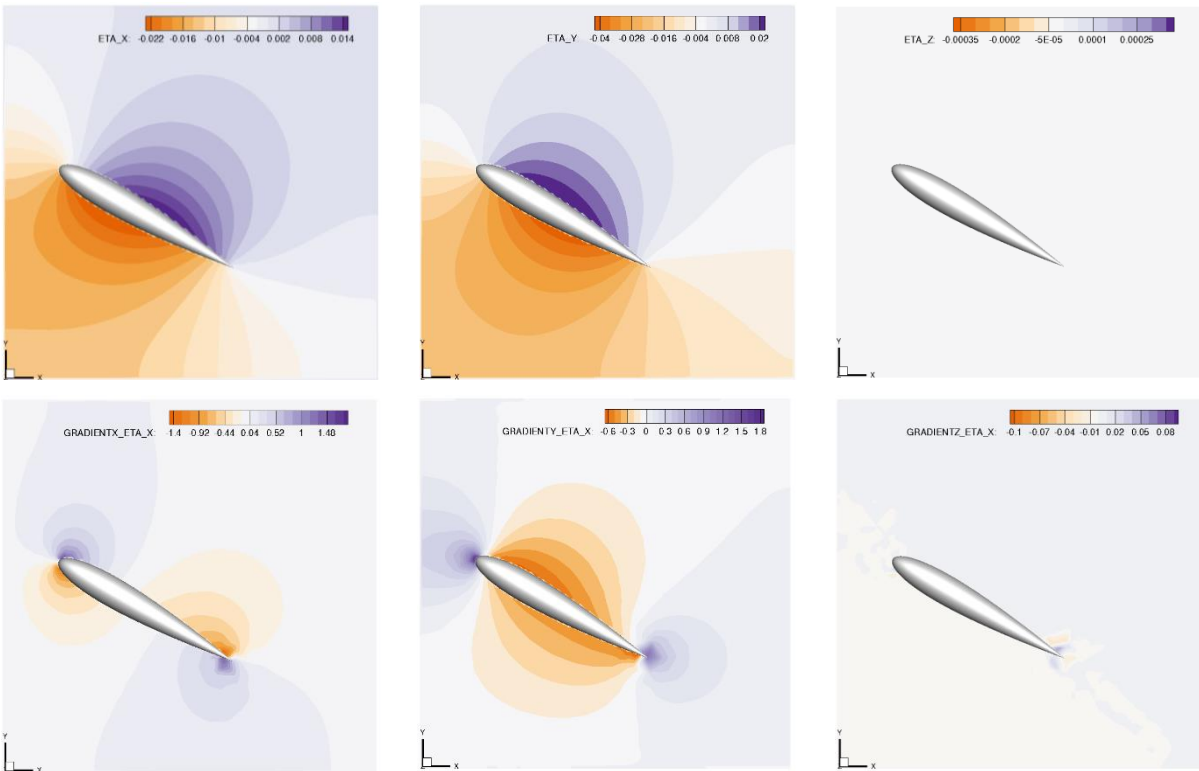

Figure 3: Harmonic functions η_x, η_y and η_z (top row) and components of the gradient $\nabla\eta_x$ (bottom row) characterizing the relative influence of the flow field in the different parts of the flow domain on the hydrodynamic force.

Once the η functions are determined, the application of equation (11) to obtain the forces from the velocity fields is straight forward. However, there is a term that requires the integration of the vorticity at the wing surface. This may add some difficulties to the computation, as the velocity fields are discretized using a rectangular grid with not enough spatial resolution to be able to determine the velocity gradients accurately in the surface of the wing. Figure 4 shows how the vorticity field is not accurate enough in the wing surface when obtained from the regular grid velocity fields.

To solve this setback, an irregular grid around the wing has been developed to obtain the desired accuracy. Then, the velocity field is interpolated into this new grid to obtain considerably more accurate spatial derivatives in the surface of the wing. For the spatial derivative in the normal direction to the wing surface, a non-centered second-order discretization is used, while for the spatial derivative in the wing curvature direction, a centered second-order discretization is used.

These schemes are shown in equations (12) and (13). With this, equation (11) can be applied using the velocity and vorticity fields to obtain the forces around the wing.
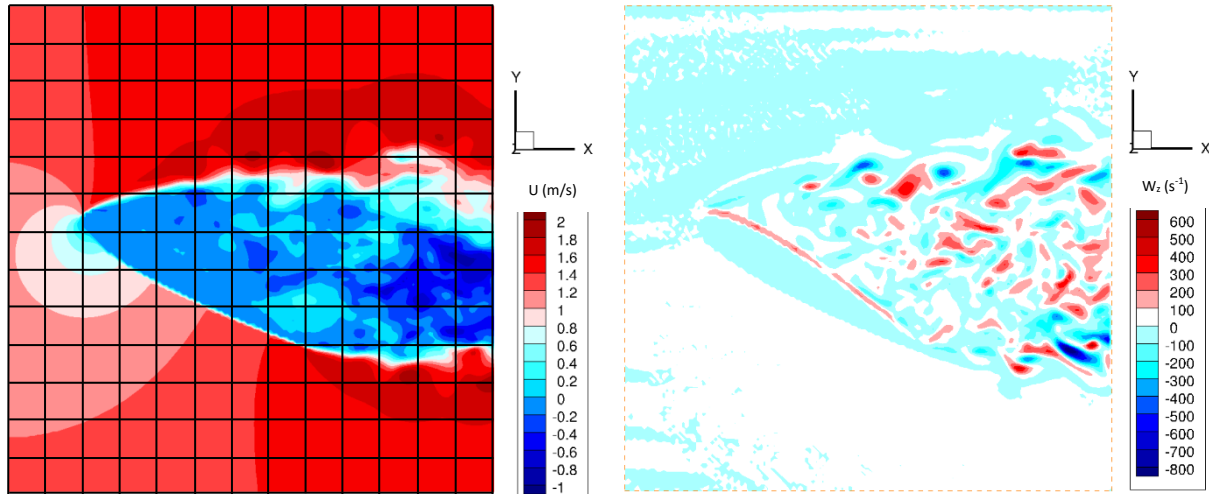

Figure 4: Velocity field in rectangular grid (left) and vorticity field obtained from it (right).
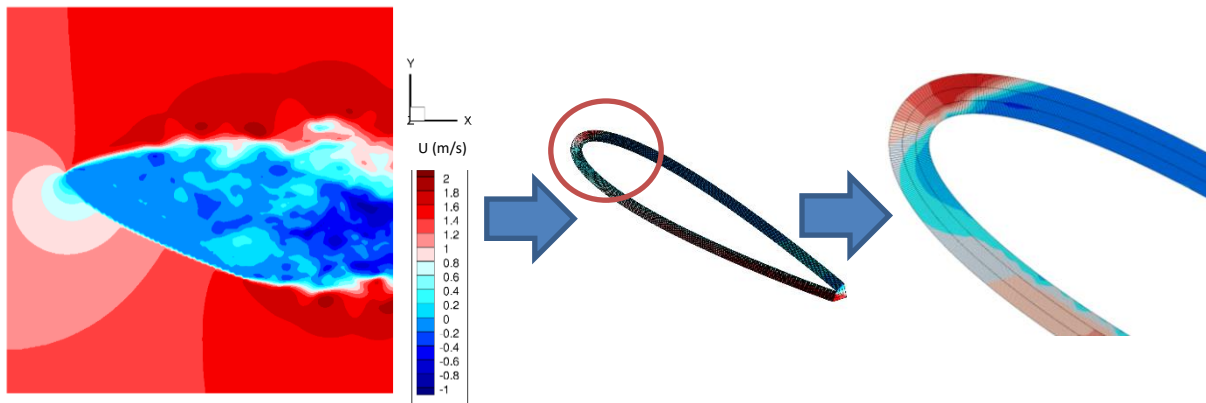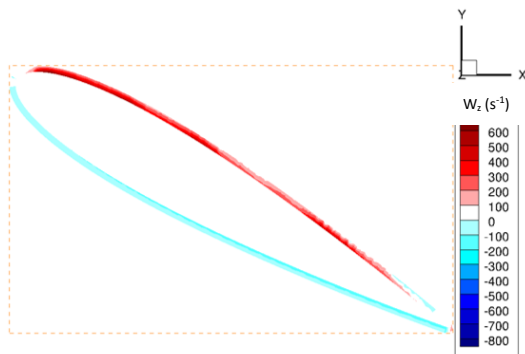

Figure 5: Schematic showing the interpolation of the velocity field to a more refined irregular grid around the wing to obtain a more accurate vorticity field on the surface.

Centered second-order discretization

$$\frac{\partial u^n}{\partial x_i} = \frac{u_{i+1}^n - u_{i-1}^n}{2\Delta x} + O(h^2) \qquad (12)$$

Non-centered second-order discretization

$$\frac{\partial u^n}{\partial x_i} = \frac{-3u_i^n - u_{i+2}^n + 4u_{i+1}^n}{2\Delta x} + O(h^2) \qquad (13)$$

Figure 6: Results of the vorticity field using the velocity interpolated into the irregular grid around the wing.

3 Results and comparison

- ## Comparison criterion

The results obtained with the different methods and parameters are compared using the relative error between them and the data base forces. By definition, the relative error is the absolute error divided by the real value:

$$\varepsilon = \frac{|F_e - F_n|}{F_n}$$

where F_e is the estimated force and F_n the numerical force from the data base.

- ## Control volume sensitivity

During the development of the variational method, high sensitivity to the size of the control volume has been noticed. For this reason, different sizes of control volumes have been studied.
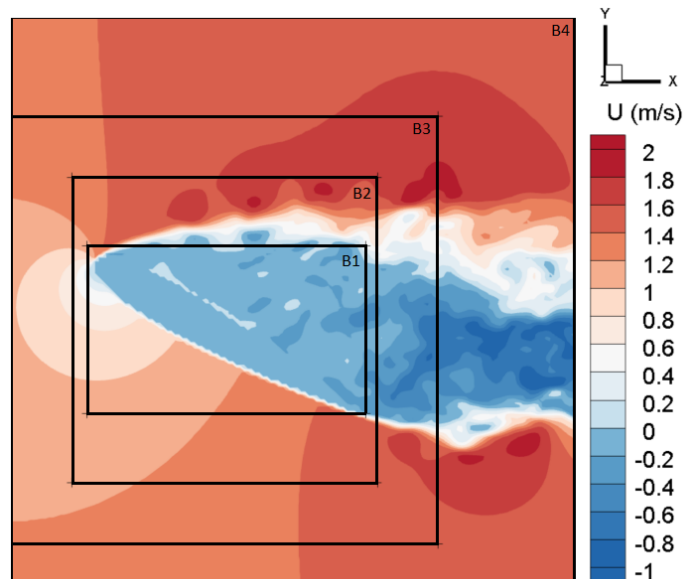

Figure 7: Representation of the different control volume sizes tested with the variational method.

Table 1: Results of the control volume sensitivity study for the variational method.

Variable	Base numérique	B1	B2	B3	B4
F_x	0.520	0.3120	0.7481	0.5357	0.5204
ε_x		39.95%	43.99%	3.11%	0.17%
F_y	0.760	0.6107	0.9512	0.6466	0.6818
ε_y		19.62%	25.19%	14.90%	10.27%

Figure 7 and table 1 show the different sizes used for the determination of the forces with the variational method and the results obtained. These results show how the error decreases when the control volume size is increased.

Looking at the solution of the η function in figure 3, which corresponds with control volume B4, it can be appreciated how the values has not converged to zero in the left and bottom sides of the volume, while in the right and top sides the values found are very close to zero. Therefore, for even smaller sizes of the control volume, such as B1 and B2, the sides of the volume are too near to the surface of the wing, having two different boundary conditions very near to each other, which makes the results obtained for the force unreliable. Nevertheless, the results obtained for the control volume B4 are promising, having less than a 1% error for the drag of the wing and a 10% error for the lift.

To show if the errors really came from having the sides of the control volumes too near to the wing, the simulation was run further to be able to export bigger velocity fields and test more sizes of control volumes. As expected, the errors were decreased having the wing far enough of the control volume walls to let the functions η converge to zero.
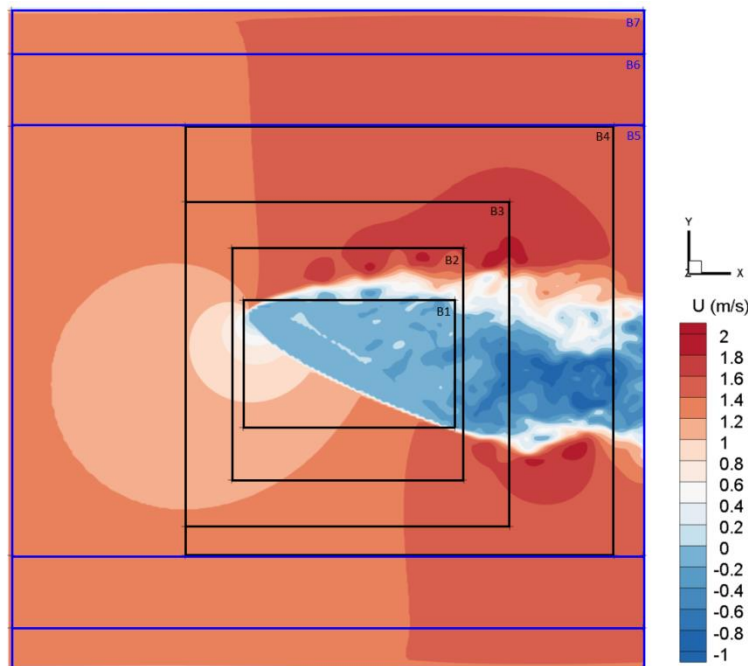

Figure 8: Representation of the new control volume sizes studied with the variational method.

Table 2: Additional results of the control volume sensitivity study for the variational method.

Variable	Base numérique	B5	B6	B7
F_x	0.5149	0.4706	0.4914	0.5030
ε_x		8.67%	4.91%	2.31%
F_y	0.7672	0.7773	0.7761	0.7865
ε_y		1.32%	1.16%	2.52%

With these last results, it is shown how the higher the size of the control volume, the better the results obtained for the aerodynamic forces of the wing. In addition, it can also be appreciated how for control volumes that have the top and bottom sides further from the object than the left and right sides, a high accuracy for the drag is obtained (example of B4). On the other hand, control volumes that have the right and left walls further from the wing than the top and bottom sides, present high accuracy for the lift (example of B5 and B6).

- **Method comparison**

The last point of this section is comparing the results obtained from the variational method for our unsteady 3D test case with the well-known momentum equation approach. Table 3 shows how the errors obtained with both methods are of the same order. This means that the choice of one approach over the other will be based on which is more suitable for the specific test of study, knowing that for the variational method an accurate enough vorticity field is required at the surface of the body and for the momentum equation approach the computation of the pressure is needed.

Table 3: Comparison between the variational method and the momentum equation approach.

Variable	Variational method (B7)	Momentum eq. approach
F_x	0.5030	0.5226
ε_x	2.31%	1.49%
F_y	0.7865	0.7475
ε_y	2.52%	2.57%

Further study of these two methods will be performed, such as an evaluation of their spatial resolution and noise sensitivity, to complete the analysis and comparison between them.

4 Conclusion

The application of the variational approach proposed by Protas et al. (2000) has been carried out to determine the unsteady aerodynamic forces in a 3D numerical test case. The main advantage of this method resides in not requiring the computation of the pressure field around the object to determine the forces. However, an accurate vorticity field is needed at the surface of the body to have reliable results.

The momentum equation approach, another non-intrusive method to determine the forces, was also applied to our test case to have a performance comparison between the two. The results showed how both methods are able to obtain the forces around the tested wing with less than a 3% error. Therefore, it will be more convenient to apply the variational method to cases in which the position of the object is known accurately, which allows to obtain a good enough vorticity field at the wing surface and it does not require the computation of the pressure. On the other hand, when the vorticity at the wing surface cannot be obtain with enough accuracy, the momentum equation approach is more suitable and the pressure computation will be required.

Further study will be carried out to determine which approach has a better performance when reducing the spatial resolution of the velocity fields and adding noise to the data. In addition, both approaches will be tested with experimental data to see the results in a real application.

Acknowledgements

References

David L, Jardin T, and Farcy A (2009) On the non-intrusive evaluation of fluid forces with the momentum equation approach. *Measurement Science and Technology* 20:1-11

Jeon Y J, Gomit G, Earl T, Chatellier L, and David L (2018) Sequential least-square reconstruction of instantaneous pressure field around a body from TR-PIV. *Experiments in Fluids* 59:27

Kurtulus D F, Scarano F, and David L (2007) Unsteady aerodynamic forces estimation on a square cylinder by TR-PIV. *Experiments in Fluids* 42:185-196

Lighthill J (1986) Fundamentals concerning wave loading offshore structures. *Journal of Fluid Mechanics* 173:667-681

Lin J C, and Rockwell D (1996) Force identification by vorticity fields: techniques based on flow imaging. *Journal of Fluids and Structures* 10:663-668

Noca F, Shiels D, and Jeon D (1997) Measuring instantaneous fluid dynamic forces on bodies, using only velocity fields and their derivatives. *Journal of Fluids and Structures* 11:345-350

Noca F, Shiels D, and Jeon D (1999) A comparison of methods for evaluating time-dependent fluid dynamic forces on bodies, using only velocity fields and their derivatives. *Journal of Fluids and Structures* 13:551-578

Protas B, Styczek A, and Nowakowski A (2000) An Effective Approach to Computation of Force in Viscous Incompressible Flows. *Journal of Computational Physics* 159:231-245

Quartapelle L, and Napolitano M (1983) Force and moment in incompressible flows. *AIAA journal* 21:911-913

Van Oudheusden B W, Scarano F, and Casimiri E W (2006) Non-intrusive load characterization of an airfoil using PIV. *Experiments in Fluids* 40:988-992